Lifting the veil on quark matter in compact stars with core g-mode oscillations

WEI WEI, ¹ MARC SALINAS, ² THOMAS KLÄHN, ² PRASHANTH JAIKUMAR, ² AND MEGAN BARRY ²

¹ College of Science, Huazhong Agricultural University, Wuhan, Hubei, P.R.China ² Department of Physics & Astronomy, California State University Long Beach, Long Beach, CA 90840, U.S.A.

ABSTRACT

Compact stars containing quark matter may masquerade as neutron stars in the range of measured mass and radius, making it difficult to draw firm conclusions on the phase of matter inside the star. The sensitivity of core g-mode oscillations to the presence of a mixed phase may alleviate this difficulty. In hybrid stars that admit quark matter in a mixed phase, the g-mode frequency rises sharply due to a marked decrease in the equilibrium sound speed. Resonant excitation of g-modes can leave an imprint in the waveform of coalescing binary compact stars. We present analytic and numeric results to assess the sensitivity displayed by g-mode oscillations to quark matter in a homogeneous or mixed phase and also compute relevant damping times in quark matter due to viscosity.

Keywords: Compact Stars, Mixed Phases, Gravitational Waves, Equation of State

1. INTRODUCTION

The discovery by the Advanced LIGO and Advanced VIRGO collaborations of the binary neutron star merger GW170817 (Abbott et al. 2017) opens a new observational window into compact star properties. Many recent works (Hu et al. 2020; Radice et al. 2018; Sieniawska et al. 2019; Abbott 2018; De et al. 2018; Chatziioannou et al. 2018; Malik et al. 2018; Tews et al. 2018; Zhu et al. 2018; Christian et al. 2019; Li et al. 2018) have explored constraints on the neutron star equation of state (EoS) using tidal polarizabilities extracted from gravitational waveforms during the late inspiral phase. It appears possible, though not conclusive, that one or both of the component stars in the merger could be hybrid stars; that is, they support a phase transition to quark matter at high density (Paschalidis et al. 2018; Nandi & Char 2018). In effect, the so-called "masquerade" problem (Alford et al. 2005) for compact stars persists: a hybrid star with quark matter in its interior is indistinguishable from an ordinary neutron star based on the current observational status, especially if quark matter is in a mixed phase with hadronic matter. A confirmation of this possibility was made in Wei et al. (2019) for nuclear to 2-flavor, 3-flavor and sequential flavor transitions. It has been suggested (Brillante & Mishustin 2014; Flores & Lugones 2014; Sotani et al.

2011, 2013) that mapping out the radial or non-radial oscillation mode frequencies can provide a clear distinction between neutron and hybrid stars, with only a weak dependence on the poorly known equation of state (EoS) of the quark phase. Given this idea, and that non-radial oscillations couple to gravitational waves, we examine a diagnostic of the phase structure of matter inside neutron stars: the core q-mode oscillations (Reisenegger & Goldreich 1992; Miniutti et al. 2003). We find that these modes are sensitive to the presence and the proportion of quark matter inside neutron stars, similar to the conclusions in Dommes & Gusakov (2016); Yu & Weinberg (2017), which focused on hyperons. However, the appearance of hyperons does not involve any phase transition, so their effect on the g-mode is less dramatic. The effect of resonant g-mode oscillations on the tidal phase accumulated during the inspiral for compact stars is probably too small to detect with the current sensitivity of gravitational wave detectors (Lai 1994; Yu & Weinberg 2017), but the effect may be more pronounced in hybrid stars, which could finally lift the veil on quark matter inside neutron stars and solve the masquerade problem.

In this paper, our focus is on the characteristics of g-mode oscillations in the quark-hadron mixed phase through a theoretical analysis of the restoring force (buoyancy) and damping. Typically, buoyancy arising from thermal and/or chemical stratification inside the star (core or crust) drives the g-mode. It can also arise due to sharp density discontinuities as a result of first or-

der phase transitions (Miniutti et al. 2003; Kruger et al. 2015). Core q-mode oscillations arising from chemical stratification carry the imprint of the fluid's composition, a feature that can potentially be exploited by gravitational wave detectors operating in the (0.1-1) kHz regime (Yu & Weinberg 2017). The g-mode is driven by the mismatch between mechanical and chemical equilibrium rates of a displaced fluid parcel, expressed by the difference between the local equilibrium and adiabatic sound speed, i.e., the Brunt-Väisälä frequency. Compared to a pure phase, a mixed phase system (ignoring surface and Coulomb forces) is more compressible due to its ability to distribute conserved charges globally. The drop in the equilibrium sound speed upon onset of the mixed phase is reflected in an increase of the q-mode frequency. This is the basic result we exploit in this paper to characterize the q-mode as a diagnostic for the phase transition to quark matter.

The g-mode for (n, p, e^{-}) matter with or without additional leptonic and hadronic species has been addressed in previous works (Reisenegger & Goldreich 1992; Lai 1994; Kantor & Gusakov 2014; Yu & Weinberg 2017; Dommes & Gusakov 2016; Zhou & Zhang 2017; Passamonti et al. 2016). For quark matter, modeldependent numerical studies have been reported (Sotani et al. 2011; Fu et al. 2017; Vásquez Flores & Lugones 2014; Ranea-Sandoval et al. 2018), but none are in the context of a mixed phase (continuous phase transition). We take a simpler but more general approach that allows for analytic estimates of the Brunt-Väisälä frequency in quark matter, and reveals the sensitivity of the g-mode to the onset and the proportion of the quark phase. The q-mode frequency vanishes in non-interacting and massless two and three (or any N_f) flavor quark matter, but can appear in any of the following realistic situations: non-zero quark mass, inclusion of interactions, a quarkhadron mixed phase. We illustrate these three cases separately for the sake of simplicity. The first and second are treated with analytic approximations, whereas for the third, we employ a common parameterization, where hadronic matter is described by a member of the family of Dirac-Brueckner-Hartree-Fock (DBHF) EoS (van Dalen et al. 2004), and quark matter is described by the vector-enhanced Bag model (vBag EoS) (Klähn & Fischer 2015). Within acceptable parameter ranges of these models, we find a steep rise in the g-mode frequency upon the appearance of a mixed phase. We discuss how this can impact tidal resonance phenomena in binary neutron star mergers where one or both components are hybrid stars with a (mixed-phase) quark matter core, and whether the effect can survive mode damping. A more detailed study of q-mode resonant coupling to dynamical tides in neutron stars and the subsequent impact on gravitational wave phasing during inspiral is left to future work.

This paper is organized as follows: sec II describes how core g-mode oscillations probe the phase structure of compact star interiors, sec III contains analytic results for the Brunt-Väisälä frequency in models of interacting nuclear and quark matter, sec IV gathers our numerical results for the g-mode jump at the onset of the mixed phase, sec V and VI discuss estimates of g-mode damping times and detectability using gravitational waves, followed by our conclusions in sec VII.

2. G-MODE OSCILLATIONS

The g-modes arising from chemical stratification are quite sensitive to the composition of dense matter. Therefore, they may be a better probe of the EoS than the f and p-modes. For example, the g-mode frequency depends on the proton fraction which is affected by the nuclear symmetry energy. The latter determines important physical quantities such as the compact star's radius, its tidal deformability and neutrino emission thresholds (Sahoo et al. 2016; Zhang & Li 2019; Krastev & Li 2019; Lattimer et al. 1991; Gandolfi et al. 2012). The symmetry energy also plays a key role in the properties of terrestrial nuclei, such as neutron skin thickness and dipole polarizabilities (Cao et al. 2015; Dong et al. 2015). As such, theoretical studies of the gmodes add to the list of diagnostics of dense matter properties coming from other phenomena in nuclear astrophysics. We emphasize that the g-mode addressed in this work is different from the crustal (Finn 1987), thermal (Strohmayer 1992) and discontinuity (McDermott 1990) g-modes, since we assume a continuous phase transition without a density discontinuity.

In order to determine the q-mode spectrum, we first construct the stellar structure using General Relativity (TOV equations). To simplify the linearized fluid perturbation equations from which we calculate the frequency of the g-mode, we employ the Newtonian and Cowling approximations, neglecting the back reaction of the Newtonian gravitational potential. While this is not strictly consistent with the fully relativistic treatment of the background structure, the impact of these simplifying approximations is not severe, typically only affecting the frequencies of the p-mode and g-mode at the 5-10% level (Gregorian 2015). However, the f-mode frequencies at low angular quantum number can be more sensitive to the Cowling approximation. To go bevond the Cowling approximation involves a considerable complication since the fluid equations must be treated in full General Relativity. While this is essential for a

self-consistent calculation of gravitational waves, here we are only trying to obtain the approximate trend in the frequency as a function of stellar parameters, not the explicit wave forms, for which the Cowling approximation is sufficient.

Accordingly, the system of equations used to compute g-mode frequencies in the neutron star are given by (Fu et al. 2017; Bildsten & Cumming 1998)

$$\frac{\partial}{\partial r}(r^2\xi_r) = \left[\frac{l(l+1)}{\omega^2} - \frac{r^2}{c_s^2}\right] \left(\frac{\delta p}{\rho}\right) \tag{1}$$

$$\frac{\partial}{\partial r} \left(\frac{\delta p}{\rho} \right) = \frac{\omega^2 - \omega_{BV}^2}{r^2} (r^2 \xi_r) + \frac{\omega_{BV}^2}{g} \left(\frac{\delta p}{\rho} \right) \qquad (2)$$

where ξ_r is the radial component of the fluid perturbation, δp the Eulerian pressure perturbation, ρ is the energy density and the Brunt-Väisälä frequency

$$\omega_{BV}^2 \equiv N^2 = g^2 \left(\frac{1}{c_e^2} - \frac{1}{c_s^2} \right)$$
 (3)

depends on the equilibrium (c_e) and adiabatic (c_s) sound speeds. The solution of the system of eqs.(1) & (2) under relevant boundary conditions, viz., regularity at the stellar center $(r \to 0)$ and vanishing of the Lagrangian pressure variation $\Delta p = c_s^2 \Delta \rho$ at the surface, can exist only for discrete values of the mode frequency ω . While we present numerical results for the f- and p-modes as well, our theoretical focus in this work is on the l=2g-modes. Also, all our results, including the estimate of the tidal overlap integral in hybrid stars, are for the g1 mode - the one with lowest radial quantum number and the highest frequency. As this mode has the largest tidal coupling coefficient and is likely to be excited late in the merger when the tidal force is stronger, we have chosen to study this mode alone. Though overtones are definitely present, we did not perform any explicit computations with those.

Once a background stellar configuration is specified, we solve eqs.(1) and (2) numerically, subject to the boundary conditions mentioned above, and pick out the g1 mode from the resulting spectrum by counting the number of nodes of the eigenfunction. We note in passing that one can perform a local analysis of these equations in the eikonal approximation, which yields (Reisenegger & Goldreich 1992)

$$\omega^2 \approx \frac{l(l+1)}{(kr)^2 + l(l+1)} N^2 \tag{4}$$

but this approximation is less accurate for low-order g-modes, so we do not use it in this work. Convectively stable g-modes exist for $N^2 > 0$, implying that

$$c_s^2 - c_e^2 = -\left(\frac{\partial p}{\partial x}\right)_o \left(\frac{dx}{d\rho}\right) > 0$$
 (5)

should be fulfilled, where $x=n_p/n_B$ is the proton-to-baryon density ratio, which equals the electron-to-baryon density ratio $Y_e=n_e/n_B$ in charge neutral (n,p,e^-) matter.

3. ANALYTIC ESTIMATES FOR SIMPLE MODELS OF DENSE MATTER

The sound speeds and g-mode frequency can be approximately calculated analytically in a few simple, and surprisingly, even interacting models of nuclear or quark As an example, we compute these quantities in interacting two flavor quark matter based on the vBag model (Klähn & Fischer 2015), which has been recently introduced to reconcile the missing features of the perturbative or thermodynamic Bag model (no chiral symmetry breaking) and Nambu-Jona-Lasinio (NJL)-type models (no confinement) within a single non-perturbative picture. This model is similar in spirit, but different in details than the more recent vMIT model (Gomes et al. 2019). The vBag model has proved to be versatile, with astrophysical applications such as mixed phases in neutron stars, protoneutron stars and supernova explosions, as demonstrated in recent works (Klähn et al. 2017; Fischer et al. 2017b,a). The purpose of studying these simple models is to emphasize the key quantities that determine the occurrence of stable g-modes, typically the nuclear or quark symmetry energy.

3.1. Nuclear Model: The DBHF Equation of State

Before we list the analytic results, we emphasize the importance of the symmetry energy in nuclear/quark matter to the g-mode. Employing the widely used functional form for the nuclear contribution to the energy per baryon (Prakash et al. 1988; Wiringa et al. 1988), $E_B(n_B, x) \approx E_0(n_B) + E_s(n_B)(1 - 2x)^2$, it follows that

$$\frac{x}{(1-2x)^3} = \frac{64E_s(n_B)^3}{3\pi^2 n_B} \tag{6}$$

for (n, p, e^-) matter in β equilibrium, where $E_s(n_B)$ is the symmetry energy of uniform matter and $E_0(n_B)$

is the energy per baryon of symmetric matter. Working in the parabolic approximation, we find

$$N \approx 2 \left(\frac{g}{c_e}\right) \left(\frac{x}{3}\right)^{1/2} \frac{(3_B n E_s^{'} - E_s)}{\sqrt{E_s(\frac{10}{9}E_0 + 2n_B E_s^{'} + n_B^2 E_s^{''})}}$$
(7

where g is the local gravitational field and primes denotes density derivatives. It is clear from this expression that the g-mode spectrum warrants further investigation to determine its sensitivity to properties of the nuclear medium. For the non-interacting (n, p, e^{-}) gas, $N \approx (g/c_e)(3x/7)^{1/2}$, which is consistent with other approximate estimates in the literature (Lai 1994; Reisenegger & Goldreich 1992). Here, we have used natural or Planck units $\hbar = c = 1$. The Brunt-Väisälä frequency in the non-interacting case $N \sim 100$ Hz. Extensions to various parameterized models of the nuclear interaction have been considered in (Lai 1994; Reisenegger & Goldreich 1992; Fu et al. 2017). In our numerical calculations, we use the nuclear EoS DBHF used in Wei et al. (2019). The proton fraction and symmetry energy as a function of baryon density is displayed for this EoS in Fig.1.

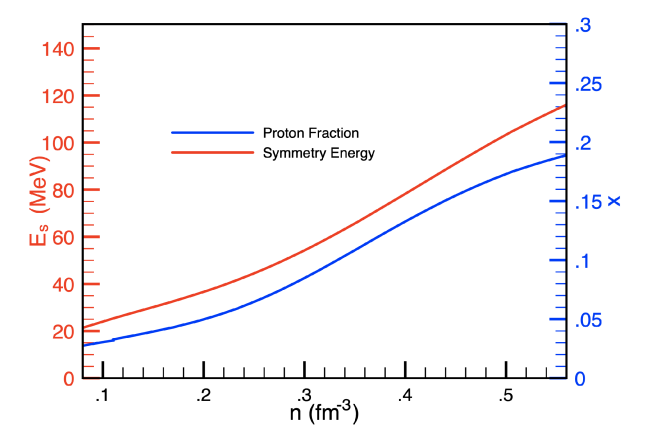


Figure 1. Symmetry energy $E_s(n_B)$ and proton fraction x for the DBHF nuclear EoS across a typical density range from the inner crust boundary to the core of the neutron star.

3.2. Quark Model I: The Thermodynamic Bag Equation of State

Since we are interested in the impact of quark matter on the g-mode, we consider some simple models of quark matter where the g-mode frequency can be estimated analytically. For non-interacting two flavor quark matter, charge neutrality and β -equilibrium pro-

vide two constraints on the up and down quark chemical potentials μ_u and μ_d . This renders the electron fraction x_e independent of the baryon density, as x_e acquires the fixed value ≈ 0.0056 , implying that $\omega_{BV}=0$, and the absence of g-mode oscillations. This situation is not realistic however, and we can imagine three different ways in which composition gradients can appear in quark matter. Firstly, the moderately heavy strange quark can appear at high density, modifying the charge neutrality condition such that $\mu_e \approx m_s^2/(4\mu_q)$, where μ_q is the quark chemical potential. Consequently, the electron fraction depends on density, providing the necessary variation of composition. Secondly, quark-quark interactions can generate $N\neq 0$, which we demonstrate in the vBag model in the two-flavor sector. In this particular model, repulsive vector interactions that support hybrid stars as heavy as $2M_{\odot}$ determine the electron fraction. Thirdly, even though non-interacting homogeneous two-flavor quark matter has a fixed electron fraction, $N \neq 0$ can occur when such matter is part of a mixed phase with nuclear matter, where the pressure varies smoothly as the quark fraction grows. We model this case a little later in this section using Wood's relation (Wilson & Roy 2008) for a mixture of compressible fluids and show that it can support q-modes. In a more detailed numerical analysis in section IV, we will employ the Gibbs construction for the mixed phase and compute the g-mode frequency therein.

For non-interacting massless two-flavor quark matter in the corresponding parabolic approximation for the energy per baryon of the quarks $E_q(n_B, x_e)$, the isospin asymmetry is given by $\delta = 1 - 2x_e = 3(n_d - n_u)/(n_d + n_u)$. The quark symmetry energy $E_s(n_B) \propto n_B^{1/3}$ which leads to a fixed value for $x_e \approx 0.0053$, within 5% of the value obtained previously with no approximation to $E_q(n_B, x_e)$. In quark matter with massive strange quarks, the symmetry energy depends additionally on the fraction of strange quarks $x_s = n_s/n_B$ (Chu & Chen 2014), wherefore $E_q(n_B, \delta, x_s) \approx E_0(n_B, x_s) + E_s(n_B, x_s)\delta^2$ leads to a system of two equations that determine $x_e(n_B)$ and $x_s(n_B)$.

$$\frac{x_e}{(1 - 2x_e - 2x_s/3)^3} = \frac{64E_s(n_B)^3}{3\pi^2 n_B}$$
 (8)

$$2 - x_e - x_s = \left(x_s^2 + \frac{m_s^2}{(\pi^2 n_B)^{2/3}}\right)^{3/2} \tag{9}$$

Therefore, the g-mode frequency, which directly involves the gradient of the composition with baryon number (or energy) density via eq.(5), serves as a probe of the symmetry energy.

Let us now address the three examples that provide for g-modes in quark matter. The first of them involves introducing the strange quark at sufficiently high density. Within the thermodynamic Bag model (henceforth, tdBag) with a Bag constant B, we can write the EoS for quark matter $P(\rho)$ to leading order in the strange quark's current mass m_s as

$$p(\rho) = \frac{1}{3}(\rho - 4B) - \frac{m_s^2}{3\pi}\sqrt{\rho - B}$$
 (10)

where p is the pressure and ρ the energy density. We can ignore the tiny contribution of the electrons to the pressure, of order m_s^8/μ_q^4 . Effectively, this means the adiabatic sound speed is given by

$$c_s^2 = \frac{1}{3} - \frac{m_s^2}{6\pi\sqrt{\rho - B}} \tag{11}$$

Eq.(5) can be recast as (Lai 1994)

$$c_s^2 - c_e^2 = -\left(\frac{n_B}{p+\rho}\right) \left(\frac{\partial p}{\partial x_e}\right) \left(\frac{dx_e}{dn_B}\right) \tag{12}$$

For the non-interacting case, an approximate solution to eqs.(8) and (9) that is accurate to better than a few percent for densities of interest yields $\mu_e \approx m_s^2/4\mu_q$. This implies that $x_e \equiv n_e/n_B \propto m_s^6/n_B^2$ so that $(dx_e/dn_B) = -2(x_e/n_B)$. Since $\mu_e/\mu_q \ll 1$, we can also approximate the quark pressure for homogeneous three-flavor quark matter as

$$p(\mu_q, \mu_e) = p_0(\mu_q) - n_Q(\mu_q)\mu_e + \mathcal{O}(\mu_e^2)$$
 (13)

with the charge density $n_Q = (\partial p/\partial \mu_e) = m_s^2 \mu_q/(2\pi^2)$. Noting that $x_e \propto \mu_e^3$, we obtain

$$\left(\frac{\partial p}{\partial x_e}\right) = \frac{m_s^2 \mu_q \mu_e}{6\pi^2 x_e} \tag{14}$$

Substituting this result in eq.(12) and using eq.(3),

$$N \approx \frac{\sqrt{3}}{2\pi} \frac{g}{c_e} \left(\frac{m_s^2}{\sqrt{\rho - B}} \right) \tag{15}$$

The difference between the adiabatic and equilibrium sound speeds is, in this case, of order m_s^4/B . For the case of a strange star, near the surface, $\rho \approx 4B$, so that $N \simeq (g/(2\pi c_e))(m_s^2/\sqrt{B})$, which is in good agreement with the estimate in Abney et al. (1996). For neutron stars with a quark core, we may conclude from eq.(15) that the resulting g-mode frequency (for low-l values) $\omega_{\rm BV} \sim 100$ Hz, which is very similar to the estimate for non-interacting (n,p,e^-) matter. However, numerical results for realistic models of nuclear and quark matter with interactions show that their g-mode frequencies are quite different (see Fig.6).

3.3. Quark Model II: The Non-perturbative vBag Equation of State

We now consider the case of a 2-flavor interacting quark model, namely, the vBag model, as an example of how interactions can induce g-mode oscillations. The vBag model is a hybrid approach that accounts for scalar interactions and hence chiral symmetry breaking by assuming bare quark masses and flavor dependent chiral bag constants $(B_{\chi,f})$ to reproduce the proper critical chemical potential for each flavor's chiral symmetry restoration. Vector interactions are taken into account non-perturbatively in analogy to the NJL model (Klevansky 1992). The quark pressure and energy density are given by

$$P_q = \sum_f P_f + B_{dc}; \quad \epsilon_q = \sum_f \epsilon_f - B_{dc}. \quad (16)$$

where B_{dc} is the confinement Bag constant, introduced to ensure that quarks are confined in the chirally restored phase. We may take it to be the same for both light flavors. The individual flavor pressure and energy density appearing in the equations above are

$$P_f(\mu_f) = P_{FG,f}(\mu_f^*) + \frac{K_v}{2} n_{FG,f}^2(\mu_f^*) - B_{\chi,f} \quad (17)$$

$$\epsilon_f(\mu_f) = \epsilon_{FG,f}(\mu_f^*) + \frac{K_v}{2} n_{FG,f}^2(\mu_f^*) + B_{\chi,f} \quad (18)$$

with the subscript FG denoting the Free Fermi gas expression. We choose $B_{\chi,u}=B_{\chi,d}$ to avoid sequential restoration, which is a more complicated scenario. These equations contain the vector repulsion term $\propto K_v$, which comes from vector current-current interactions and is connected to the gluon mass scale in Dyson-Schwinger studies of non-perturbative QCD. The repulsion term is essential to stiffen the quark equation of state, and support compact stars at least as heavy as $2M_{\odot}$. We will see that it also controls the electron fraction in quark matter, thereby influencing the g-mode. The introduction of the vector term also modifies the quark number densities and chemical potentials as:

$$\mu_f = \mu_f^* + K_v n_{FG,f}(\mu_f^*) \tag{19}$$

$$n_f(\mu_f) = n_{FG,f}(\mu_f^*) \tag{20}$$

The vBag equation of state can be expressed as:

$$P_q = \frac{1}{3} (\epsilon_q - 4\sum_f B_{\chi,f}) + \frac{4}{3} B_{dc} + \frac{K_v}{3} \sum_f n_f^2(\mu_f) . \tag{21}$$

which has a non-barotropic form since $n_f(\mu_f)$ encodes composition information. Charge neutrality requires

 $(2/3)x_u-(1/3)x_d-x_e=0$, where $x_i=n_i/n_B$ are the quark to baryon number fractions of species i. We also impose β -equilibrium: $\mu_d - \mu_u = \mu_e$. Since $x_u + x_d = 3$, we can obtain $x_e(n_B)$ numerically from these conditions. It is useful to note that the depressed cubic eq.(19) has the solution

$$\overline{\mu^*}_f = \sinh\left(\frac{1}{3}\sinh^{-1}\left(3\bar{\mu}_f\right)\right) \tag{22}$$

with the scaling $\bar{\mu} = (\sqrt{3K_v}/(2\pi)) \mu$. Subsequently, we obtain an analytic approximation for the electron fraction, which is within 5% of the numerical result.

$$x_e(n_B) = \frac{\left[\tilde{n} + (2^{1/3} - 1)(\pi^2 \tilde{n})^{1/3}\right]^3}{3\pi^2 \tilde{n}}$$
 (23)

$$\tilde{n} = K_v^{3/2} n_B \tag{24}$$

For values in the typical parameter range $K_v \sim (2\text{-}6)$ GeV⁻², the dimensionless baryon density is $\bar{n} \sim (0.002\text{-}0.02)$ for densities of relevance to quark matter in compact stars $(n_B \sim (3\text{-}6)n_{\text{sat}})$, implying that $x_e \sim (0.006\text{-}0.014)$. To obtain the difference in sound speeds from eq.(12), we note that (with p, E denoting the total pressure and energy per baryon from quarks and electrons)

$$\frac{\partial p}{\partial x_e} = n_B^2 \frac{\partial}{\partial n_B} \frac{\partial E}{\partial x_e} = n_B^2 \frac{\partial}{\partial n_B} \left[\mu_e + \mu_u - \mu_d \right] \quad (25)$$

Expressing the chemical potentials μ_i in terms of the partial fractions x_i , we arrive at

$$\frac{\partial p}{\partial x_e} = -\frac{2}{3} n_B^2 K_v (1 - 2x_e) \tag{26}$$

From eq.(23) and (24), it follows that

$$n_B \frac{dx_e}{dn_B} = \frac{2K_v}{(3\pi^2)^{1/3}} (n_B x_e)^{2/3}$$
 (27)

From eqs.(26) and (27), and to leading order in x_e , we find

$$c_s^2 - c_e^2 \approx \frac{x_e^{2/3}}{(3\pi^2)^{1/3}} \left(\frac{K_v^2 \, n_B^{8/3}}{\sum_f (\epsilon_{FG,f}(\mu_f^*) + \frac{3}{4} K_v \, n_{FG,f}^2(\mu_f^*))} \right)$$
(28)

To the same order in x_e , the Brunt-Väisälä frequency in this model is

$$N \approx \frac{g \, x_e^{1/3}}{c_e} \, \times \tag{29}$$

$$\left(\frac{K_v n_B^{4/3}}{\sqrt{(P_q + \epsilon_q) + 2\sum_f (K_v n_{FG,f}^2(\mu_f^*) + B_{\chi,f}) - B_{dc}}}\right)$$

Finally, we consider the case of a mixed phase of non-interacting 2-flavor quark matter with nuclear matter, which also implies the existence of g-mode oscillations. This foreshadows the more realistic numerical treatment of the mixed phase in the next section.

As an analogy, consider an admixture of two (uncharged) components such as water and air. Even at very low bubble fraction χ , the effective incompressibility is reduced sharply since the density of the mixture is hardly changed, whereas air bubbles significantly reduce the pressure compared to a pure liquid. The resulting equilibrium sound speed is given by (Wood 1930)

$$\frac{1}{c_{\rm mixed}^2} = \frac{(1-\chi)^2}{c_l^2} + \frac{\chi^2}{c_g^2} + \chi(1-\chi) \left(\frac{\rho_g}{\rho_l \, c_l^2} + \frac{\rho_l}{\rho_g \, c_g^2} \right) \ (30)$$

where l and g stand for the liquid (dense) and gas (void) phase respectively. This assumes that the bubble can exchange heat with the surrounding fluid fast enough during the perturbation to maintain equilibrium. Since the material density $\rho_g \ll \rho_l$, a distinct drop in the equilibrium sound speed is seen at the onset of the mixed phase.

For a quark-hadron mixed phase, eq.(30) is not directly applicable since each phase also carries charge such that the system is globally neutral, with the void fraction given by $\chi_q = n_Q^h/(n_Q^h - n_Q^q)$ where n_Q denotes the charge density, and q and h refer to quark and hadron phases. Furthermore, the energy density ρ_q and ρ_h are similar in magnitude unlike for air and water, which would imply $c_{\rm mix} \approx c_h$ for small χ . Taking the two conserved quantities (baryon number and charge) into account, we have

$$c_{\text{mix}}^2 = \frac{dp_{\text{mix}}(\mu_B, \mu_Q)}{d\rho} = \frac{\partial p_{\text{mix}}}{\partial \mu_B} \left(\frac{d\mu_B}{d\rho}\right) + \frac{\partial p_{\text{mix}}}{\partial \mu_Q} \left(\frac{d\mu_Q}{d\rho}\right)$$
(31)

Accordingly, an additional contribution to eq.(30) exists, with the energy densities ρ_q and ρ_h replaced by the respective charge densities ρ_q^Q and ρ_h^Q respectively. As shown in Glendenning (1992) with an explicit quark-hadron mixed phase construction, the first term in eq.(31) is continuous with density at the onset of the mixed phase, but the second term involving the charge chemical potential is not. Therefore, we expect, as confirmed by our numerical results presented in sec IV, that $c_{\rm mix}$ has a negative discontinuity at the onset of the mixed phase, in effect lowering the equilibrium sound speed. The physical meaning is that the system is more compressible in a charge separated state, as internal forces have the freedom to rearrange charges between the two phases to minimize the free energy. In effect,

global charge neutrality makes the system more compressible. We note that this effect is not specific to the quark-hadron mixed phase, it will arise whenever a mixed phase is encountered in the depths of a compact star. Our numerical calculations show a similar sharp drop in the equilibrium sound speed at the onset of the mixed phase, with only a small change in the adiabatic sound speed. Therefore, $c_s^2-c_e^2>0$ and stable g-modes can be found.

4. NUMERICAL RESULTS FOR G-MODES IN THE MIXED PHASE

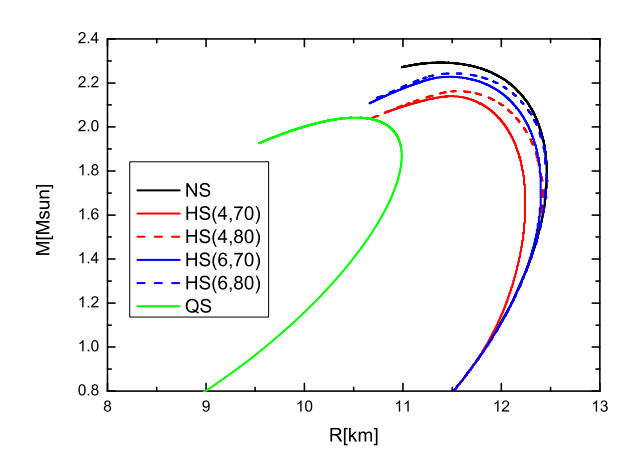


Figure 2. The mass-radius curve for three different compact star configurations - neutron stars (DBHF), hybrid stars and quark stars (vBag). The parameters of quark matter for the quark/hybrid star 1 are $B_{\rm eff}$ =70 MeV fm⁻³ and for hybrid star 2, $B_{\rm eff}$ =80 MeV fm⁻³. Variations due to vector coupling K_v =4×10⁻⁶ MeV⁻² and K_v =6×10⁻⁶ MeV⁻² are displayed.

We now examine the g-mode in the mixed phase using a realistic model for the nuclear phase (DBHF EoS) and the vBag model for the 2-flavor quark phase. Details about these EoS are given in Wei et al. (2019), also in Klähn & Fischer (2015); Klähn et al. (2017); Cierniak et al. (2018); Wei et al. (2019). Here, we employ parameters for the vBag model that yield a maximum mass of at least $2M_{\odot}$, and result in the appearance of a mixed phase of nuclear and two-flavor quark matter in the interior of neutron stars. As explained in our paper (Wei et al. 2019) on the masquerade problem, it is possible to consider two phase transitions, the first involving only (u,d) quark matter, and the second involving s-quarks at a higher density. One could also choose vBag parameters to have only three-flavor matter in a mixed phase. In either of these two more involved cases, we expect that our conclusions about the rise in g-mode

frequency would not change qualitatively, but we do not study them numerically here.

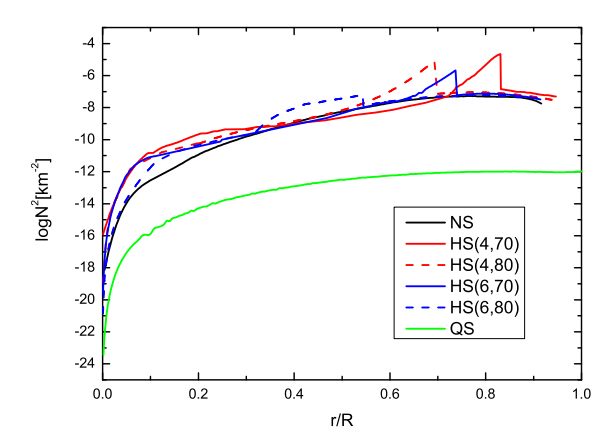


Figure 3. The local Brunt-Väisälä frequency for neutron/quark/hybrid stars plotted as a function of the relative distance from the center r/R. The parameters are same as in Fig.2. The mass of the chosen neutron and hybrid stars are $2.1M\odot$ and the mass of the quark star is $1.9M\odot$.

In Fig.2, which shows the mass-radius curve for neutron, quark and hybrid stars with our chosen EoS, we observe that the onset of the softening due to the appearance of the mixed phase happens at higher stellar mass as B_{eff} is increased, contributing to the masquerade effect that was described extensively in Wei et al. (2019). The vector interaction provides the necessary stiffness to generate masses above $2M_{\odot}$. The value of B_{eff} is also constrained by the requirement that nuclei must be stable against deconfinement to (u,d) matter in vacuum. In the vBag model, the value of B_{eff} that allows deconfinement to (u,d) matter in vacuum has a value of 60 MeV fm⁻³ at zero vector repulsion and somewhat lower at higher values of this repulsion. Our chosen values of Beff of 70 and 80 MeV fm⁻³ avoid this unphysical outcome while still permitting a phase transition to 2-flavor matter at high baryon density. From Fig.2, it is clear that vBag model parameters can be chosen so as to mask the effect of the phase transition in the mass-radius curve, so we look to the q-mode signature instead. In Fig. 3, we show the Brunt-Väisälä frequency in the star from outer core to the center. To obtain positive values of N^2 (i.e., $\log(N^2)$ real) throughout the core, as required by the lack of convection in cold compact stars, we found it necessary to smooth the DBHF EoS data before computing the sound speeds. which involve derivatives of the pressure with respect to energy density. The peak signals an abrupt rise of the

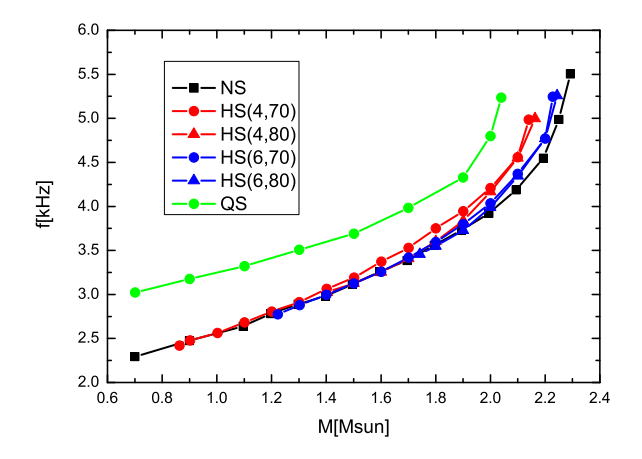


Figure 4. The Newtonian eigenfrequencies of f-modes for the neutron star, hybrid star and quark star as a function of stellar mass. Parameters are same as in Fig.2.

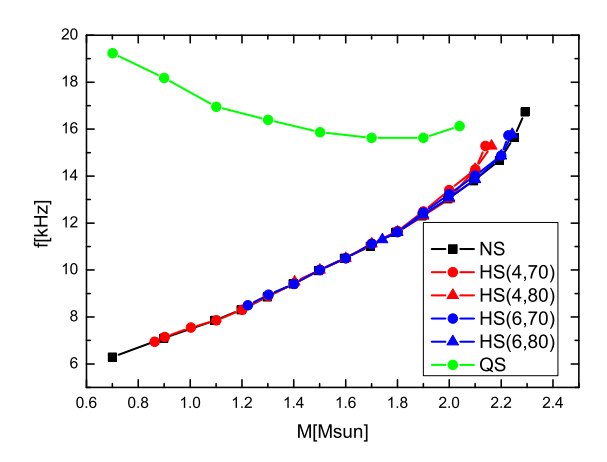


Figure 5. The Newtonian eigenfrequencies of *p*-modes for the neutron star, hybrid star and quark star as a function of stellar mass. Parameters are same as Fig.2. The trend of the *p*-mode frequency for the quark star, which is opposite that of the neutron and hybrid star, arises because the quark star is self-bound.

Brunt-Väisälä frequency inside the star due to the drastic reduction in the equilibrium sound speed, revealing the onset of the mixed phase. Although this is a continuous phase transition with no sharp density jump, the g-mode frequency is seen to rise sharply at this point for the reason explained at the end of the previous section. In Figs. 4, 5 and 6, we observe the impact of the phase transition on the fundamental f, p, g-modes.

While the f and g-modes both have frequencies within the sensitivity range of Advanced LIGO/Advanced

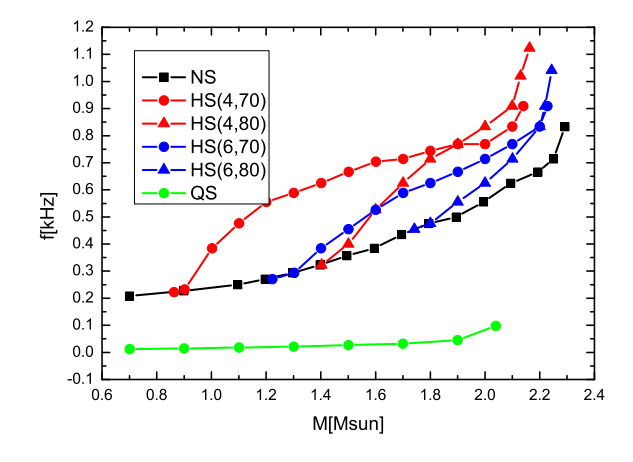


Figure 6. The Newtonian eigenfrequencies of g-modes for the neutron star, hybrid star and quark star as a function of stellar mass. Parameters are same as Fig.2. Note the abrupt change in slope of the g-mode frequency curve as soon as the mixed phase is favored.

VIRGO (with the g-modes more so), only the g-modes show a trend for hybrid stars that is very different from neutron stars/bare quark stars. The f-modes for hybrid stars appear to interpolate between the neutron star and quark star as we go to increasing mass. The g-modes for the hybrid star on the other hand can have frequencies much higher than either the neutron star/quark star. It is surprising that a local change in the Brunt-Väisälä frequency can impact the g1 mode frequency, given the latter's large wavelength which is comparable to the stellar radius. However, the phase fraction of quark matter rises very fast at the onset of the mixed phase, causing dramatic compositional gradients that drive the sound speed difference (and hence the Brunt-Väisälä frequency) to higher values than for ordinary neutron stars. Compared to say, the change in sound speed when muons or hyperons enter Dommes & Gusakov (2016), the fall in sound speed when quarks enter is several times larger. As a result, the magnitude of the change in the Brunt-Vaisala frequency is also much larger when the mixed phase begins. The logarithmic scale on the vertical axis of Fig.3 gives an idea of this effect. The large magnitude of this shift with respect to a normal or pure phase counters the fact that it is a local effect, resulting in a significant g-mode frequency shift nevertheless. The parameter set HS(4,70) yields the most compact configuration of all, as seen in Fig.2. Quark matter appears at the lowest density in this case, softening the equation of state the most and strongly decreasing the sound speed. Consequently, we see the largest g-mode frequency shift for HS(4,70).

Even if the compact star's mass is not measured, a q-mode frequency of about 0.8 kHz or more is likely to be supported only in a hybrid star. Within our chosen model, this also constrains the stellar mass to be above $2.0M_{\odot}$, so it could be a way to identify the most massive compact stars. We also note that lower g-mode frequencies (0.4-0.8 kHz) could originate from low/intermediate mass hybrid stars or high-mass neutron stars. These two possibilities can be distinguished if the f-mode frequency, which is very different for low and high mass stars irrespective of model parameters, is also measured. Therefore, even in the absence of a mass measurement, it is possible to extract information on the interior composition of the compact star such as whether it can support a phase transition to quark matter, using its oscillation spectrum. If the mass is known to better than a few % (Lattimer et al. 2019) and the frequency to better than few tens of Hz (Pratten et al. 2020), we can begin to constrain the parameters of the quark model which derive from the non-perturbative sector of the strong force. It is also worth noting that while the g-mode and the p-mode frequencies are both quite distinct between neutron stars and pure quark stars, only the g-mode frequencies would be in the sensitivity band of currently operational detectors. In the next section, we estimate the q-mode damping time as this affects the likelihood of practically detecting these modes with gravitational wave interferometers.

5. DAMPING TIMES FOR THE G-MODE IN QUARK MATTER

In this section, we provide estimates for the damping time of the q-mode in two-flavor quark matter, to provide some comparison with ordinary neutron stars. These are only order of magnitude estimates that can be refined by utilizing the g-mode wave functions obtained from the solution of the fluid perturbation equations along the lines of Lai (1994). However, that is beyond the scope of the current paper. Three sources of damping are identified in Reisenegger & Goldreich (1992): neutrino damping (bulk viscosity), damping by shear viscosity and gravitational wave damping (the latter being negative corresponds to mode growth). We address these in turn. Neutrino damping of the g-mode involves the relaxation of the departure from chemical equilibrium $\delta\mu(n_B, x_e) = \mu_d - \mu_u - \mu_e$ due to the nonequilibrium β -decay rate. Working at fixed baryon density, we define the typical relaxation timescale through

$$\tau_{\beta} \equiv 1/\Gamma_{\rm rel}; \quad \dot{\xi} = -\Gamma_{\rm rel}\xi; \quad \xi = \frac{\delta\mu}{T}$$
(32)

Adopting the expression for $\Gamma_{\text{rel}} = \Gamma_{d \to u + e + \bar{\nu}_e} - \Gamma_{u+e \to d+\nu_e}$ from Anand et al. (1997), we obtain

$$\tau_{\beta}(yr) \approx 8.2 T_9^{-4} \left(\frac{n_{\text{sat}}}{n_B}\right)^{2/3} \frac{1}{(\delta \mu/\text{MeV})}$$
 (33)

where $n_{\rm sat}=0.154~{\rm fm^{-3}}$ is the nuclear saturation density, and we have assumed $K_v=4~{\rm GeV^{-2}}$. The magnitude of $\delta\mu$ depends on the amplitude of the oscillation, which is uncertain, but we may assume an upper limit of $\delta\mu\approx 1~{\rm MeV}$, which corresponds to fluctuations in the chemical potentials at the 1% level. Since the oscillation timescale for the g-mode in quark matter is $\sim 0.01-0.1$ seconds, it is clear from eq.(33) that unless $T>10^{11}{\rm K}$, the g-mode is not damped by this mechanism. Even assuming tidal heating during the inspiral, the temperature is insufficient to damp the g-mode in quark matter through off-equilibrium β decays. Turning to the damping timescale from shear viscosity, recent work (Reisenegger & Goldreich 1992; Lai 1999)

$$\tau_{\rm visc}({\rm yr}) \sim \frac{L^2}{\nu} \approx 1.5 \times 10^3 L_6^2 T_9^{5/3} \left(\frac{n_{\rm sat}}{n_B}\right)^{5/9}$$
(34)

where ν is the kinematic viscosity, related to the shear viscosity as $\nu = \eta/\rho$, and we have used the shear viscosity for quark matter given in Heiselberg & Pethick (1993), which takes Landau damping into account for the gluons. $L_6 = L/(10^6 \, \mathrm{cm})$ where L is a typical wavelength scale of oscillation. This timescale is too large to damp the g-mode by itself unless $T_9 \lesssim 10^{-3}$, i.e, unless $T \lesssim 10^{-6} \, \mathrm{K}$, which is the case only for very old neutron stars.

Finally, we can estimate the effect of the secular instability of the g-mode in rotating configurations due to gravitational wave emission, also known as the CFS instability (Chandrasekhar 1970; Friedman & Schutz 1975). The low frequencies of the g-mode in quark matter implies that the critical rotation speed at which the CFS instability can be triggered in pure quark stars is $\Omega_s \sim 10-100$ Hz. When the mixed phase enters and the g-mode frequency rises sharply, stability can be restored. From the analysis in Lai (1999), we estimate

$$\tau_{\rm gw}({\rm yr}) \sim \frac{1+\mathcal{E}}{25} \hat{\omega}_i^{-5} \hat{\omega}_r \frac{R_{10}^4}{M_{14}^3} \left(\frac{10^{-4}}{\delta D_{22}}\right)^2$$
 (35)

where $\hat{\omega}_i$ and $\hat{\omega}_r$ are normalized mode angular frequencies in the inertial and rotating frames respectively, δD_{22} is the mass quadrupole and \mathcal{E} is a sub-leading contribution to the g-mode energy. Mode instability in the inviscid case sets in when ω_i turns negative, which happens at a critical spin frequency of $\nu_s \approx 0.68 \,\nu_0$ (Lai 1999), where ν_0 is the mode frequency.

Applying eq. (35) to our quark model EoS for a $1.4M_{\odot}$ star, for which $\delta D_{22} \approx .0008$ and $\mathcal{E} \approx 0.7$, we estimate the mode damping timescale to be $\tau_{\rm gw} \sim 10^3$ yrs at zero rotation for a pure quark star and $\tau_{\rm gw} \sim 10^{-2}$ yrs for a hybrid star with a mixed phase quark core. This large difference in damping times is due to the much higher g-mode frequency in the mixed phase configuration. Taking viscous damping and rotation into account, the overall damping timescale τ , which is given by

$$\tau = (\tau_{\beta}^{-1} + \tau_{\text{visc}}^{-1} + \tau_{\text{gw}}^{-1})^{-1}$$
 (36)

implies that the g-mode can be unstable to gravitational wave emission (i.e, $\tau<0$) in the temperature range $10^8{\rm K}\!\!< T<10^9{\rm K}$ for a stellar rotation frequency of about twice the frequency of the g-mode frequency at zero rotation $\approx 200~{\rm Hz}$. With decreasing rotation speed, the instability window narrows and ultimately closes. However, at slower rotation speeds, additional sources of damping such as mutual friction could become important if the quarks are in a superfluid phase.

6. DETECTING G-MODES WITH GRAVITATIONAL WAVES

How can we observe the predicted effect? If the g-mode is resonantly excited by tidal forces during the late stages of binary inspiral, the resulting energy transfer from the orbital motion to the star via tidal coupling can affect the phase of the gravitational waveform. To estimate this effect, we computed the orbital phase shift $\Delta\Phi(\tau)$ induced by a tidal resonant excitation of the principal g-mode using Eq.(21) of Reisenegger & Goldreich (1994) (with l=m=2)

$$\Delta\Phi(\tau) \approx 2 \times 10^{-2} \left[\frac{0.33}{\tau^{3/8}} - 1 \right] \left(\frac{\omega_g}{2\omega_{\rm dyn}} \right)^{-1/3} \left(\frac{S}{10^{-2}} \right)^2$$
(37)

with τ the time to coalescence (in seconds), $\omega_q = 2\pi f$ the g-mode angular frequency, $\omega_{\rm dyn} = \sqrt{GM/R^3}$ and S $\propto \langle P_{lm} | \xi^{nlm} \rangle$ with $|P_{lm}\rangle = \nabla (r^l Y_{lm}(\theta, \phi))$ is an overlap integral that quantifies the coupling of the g-mode to the 2^l -pole component of the forcing tidal field. The overlap integral in eq.(37) is computed from the solution of eqs.1 and 2, and is scaled to its typical value for a $(1.4+1.4)M_{\odot}$ binary, assuming vBag parameters that generate a hybrid star. We obtain $\Delta\Phi(\tau)\sim\mathcal{O}(1)$ radian for $\tau \sim 10$ milliseconds, which is about when the g1 mode is excited. Compared to core q-modes in a pure neutron star (Reisenegger & Goldreich 1994), the phase error for hybrid stars is larger since the overlap integral S is an order of magnitude larger for the latter. Previous similar works (eg., (Lai 1994; Yu & Weinberg 2017)) obtained $S \approx 10^{-3} - 10^{-2}$ for neutron stars with or without

superfluidity, whereas we find $S \approx 10^{-2} - 10^{-1}$ for hybrid stars. This difference is due to the presence of the mixed phase which makes the matter more compressible, increasing the amplitude of the density perturbation there and increasing S. Furthermore, the adiabatic sound speed in the mixed phase (at a given density) is smaller than for a uniform nuclear phase, which also acts to increase the density perturbation. In the case of neutron stars, we recover S about 0.01 or smaller, while $S \sim 0.1$ is possible in hybrid stars for the softest parameter set HS(4,70), potentially yielding a tidal phase error of order one. While this is promising, one still has to overcome the statistical phase error for an event given that there are still about 10 other parameters of the binary that can impact the orbital phase during inspiral. For a tidally excited resonance, using $\Delta \phi_{\rm stat} \approx \sqrt{D-1}/({\rm SNR})$, where D is the number of parameters and SNR is the signal-to-noise ratio, a conservative estimate is SNR ≥ 30 at frequencies $f \approx 0.5$ kHz. For a single detector (LIGO) at current sensitivity, this implies a nearby event (luminosity distance~40 Mpc or less, similar to GW170817), but with a network of detectors (Yang et al. 2018) or even the A+ upgrade to LIGO, there should be a much better chance of detecting the q-mode. The growth (or damping) of the q-mode in hybrid stars is also relevant to the question of detection. Once excited, the g-mode can become become secularly unstable if its growth timescale is much shorter than the viscous damping timescale in the temperature range $T \approx 10^{10} \text{K}$ that is reached just before the merger (Meszaros & Rees 1992). The growth timescale $\tau_{\rm gw} \sim 10^{-2}$ yrs from eq.(35). The damping timescales from viscosity in mixed phases inside neutron stars have not been calculated precisely, but our estimates in the previous section suggest that the damping timescale of the g-mode due to bulk viscosity is longer than the gravitational wave timescale τ_{gw} for typical merger temperatures and rotation speeds. This implies that any g-mode excited pre-merger can grow to large amplitude, beyond which it is likely to be damped due to the effect of higher temperature or non-linear effects. The g-mode may be excited post-merger as well, but their nature (thermally or discontinuity-driven) is different than the ones considered here. Another distinct possibility is the superfluid q-modes, which can be excited during coalescence (Yu & Weinberg 2017), depending on the particle species in the star's core. Based on these estimates, it would appear that the q-mode is likely to be detectable once ongoing improvements in sensitivity of gravitational wave detectors are complete. The g-modes could also have an observable electromagnetic signature, since the maximum energy absorbed by the mode (Reisenegger & Goldreich

1994)

$$\Delta E(\text{ergs}) \approx 7 \times 10^{49} \left(\frac{\omega_g}{2\omega_{\text{dyn}}}\right)^{-1/3} \left(\frac{S}{10^{-2}}\right)^2$$
 (38)

is four orders of magnitude larger than the steady state Poynting luminosity of a merging binary integrated over the resonance timescale of the g-mode (Fernandez & Metzger 2016). If even 1% of the mode energy couples to the magnetic field, it could be released in the form of hard X-ray precursors to short gamma-ray bursts or non-thermal emission.

7. CONCLUSIONS

Based on our study of core g-modes in compact stars with and without quark matter, we conclude that the frequency of these modes is very sensitive to the presence of a mixed phase containing quarks and hadrons. The equilibrium sound speed drops sharply at the boundary of the mixed phase, raising the local Brunt-Väisälä frequency and the fundamental g-mode frequency of the star. If this mode can be resonantly excited during the late stages of binary inspiral, the resulting energy transfer from the orbital motion to the star via tidal coupling can affect the phase of the gravitational waveform, or couple to electromagnetic precursors, possibly giving a signature of the quark-hadron phase transition in the star. Previous works have examined the accumulated phase error from tidal coupling to the g-mode for ordinary neutron stars with composition gradients (but no phase transition) and concluded that it is about two orders of magnitude too small to be detected by current detectors (Lai 1994; Yu & Weinberg 2017; Xu & Lai 2017). However, if one or both stars support a mixed phase of quark-hadron matter, there are really two fluid components inside each star that can be tidally forced. This, and the fact that the spectrum of q-mode is shifted to higher frequencies and is about 5 times more dense ¹ than for ordinary neutron stars, imply that more modes can become resonant as the signal sweeps through the bandwidth of the detector and possibly accumulate a larger phase error. Yu & Weinberg (2017) studied this effect in superfluid neutron stars and found that since higher frequency modes are excited later in the merger,

there is effectively no enhancement of the phase error compared to ordinary neutron stars. To determine if a similar cancellation occurs for hybrid stars, one must perform a detailed calculation of the mode amplitude evolution, energy transfer and the resulting phase error in the case of a hybrid star. All we can say based on our calculation is that g-modes from hybrid stars may lead to a larger tidal phase error than that in an ordinary neutron star due to the larger coupling coefficient for the former.

There are a few more physical effects that can alter our results quantitatively, which have not been taken into account. Rotation and full general relativity have not been incorporated at the level of the perturbative analysis. Non-linear mixing between p and q-modes due to tidal coupling is possible (Weinberg 2016) without any resonant excitation, and this can also impact the orbital dynamics and tidal phasing. This effect seems to be disfavored by the data on GW170817 (Reves & Brown 2020; Abbott et al. 2019) but only for extreme values of the p-q parameters. Other nuclear EoS parameterizations and the possibility of strange quarks appearing together or at a higher density than the light quarks would change the sound speed profile and hence the gmode frequency. Therefore, we refrain from making any bold statements on the quantitative impact of the effect proposed here on the gravitational wave signal from binary mergers. However, given the subtle nature of the masguerade problem and optimism for increased statistics on binary mergers from the next observing runs of Advanced LIGO/VIRGO as well as next generation detectors, the g-mode is a promising diagnostic for the quark-hadron phase transition deserving of further investigation.

ACKNOWLEDGMENTS

W.W. is supported by the Natural Science Foundation of China under Grant No.11903013 and China Scholarship Council. P.J. is supported by the U.S. NSF Grant No. PHY 1608959 and PHY 1913693. We thank Bryen Irving for helpful input and discussions.

REFERENCES

Abbott, B., et al. 2017, Phys. Rev. Lett., 119, 161101, doi: 10.1103/PhysRevLett.119.161101

Abbott, B. P., Abbott, R., Abbott, T. D., et al. 2019, PhRvL, 122, 061104,

doi: 10.1103/PhysRevLett.122.061104

 $^{^1}$ We find 2 distinct g-modes between 100 Hz - 1.5 kHz for neutron stars and 10 distinct modes in the same frequency range for hybrid stars.

- Abbott, B. P. e. a. 2018, Phys. Rev. Lett., 121, 161101, doi: 10.1103/PhysRevLett.121.161101
- Abney, M., Epstein, R. I., & Olinto, A. V. 1996, Astrophys. J. Lett., 466, L91, doi: 10.1086/310171
- Alford, M., Braby, M., Paris, M. W., & Reddy, S. 2005, Astrophys. J., 629, 969, doi: 10.1086/430902
- Anand, J. D., Goyal, A., Gupta, V. K., & Singh, S. 1997, The Astrophysical Journal, 481, 954. http://stacks.iop.org/0004-637X/481/i=2/a=954
- Bildsten, L., & Cumming, A. 1998, The Astrophysical Journal, 506, 842.
 - http://stacks.iop.org/0004-637X/506/i=2/a=842
- Brillante, A., & Mishustin, I. N. 2014, EPL, 105, 39001, doi: 10.1209/0295-5075/105/39001
- Cao, L.-G., Roca-Maza, X., Col, G., & Sagawa, H. 2015, Phys. Rev., C92, 034308, doi: 10.1103/PhysRevC.92.034308
- Chandrasekhar, S. 1970, Physical Review Letters, 24, 611, doi: 10.1103/PhysRevLett.24.611
- Chatziioannou, K., Haster, C.-J., & Zimmerman, A. 2018, Phys. Rev., D97, 104036, doi: 10.1103/PhysRevD.97.104036
- Christian, J.-E., Zacchi, A., & Schaffner-Bielich, J. 2019, PhRvD, 99, 023009, doi: 10.1103/PhysRevD.99.023009
- Chu, P.-C., & Chen, L.-W. 2014, ApJ, 780, 135, doi: 10.1088/0004-637X/780/2/135
- Cierniak, M., Klähn, T., Fischer, T., & Bastian, N.-U. 2018, Universe, 4, 30, doi: 10.3390/universe4020030
- De, S., Finstad, D., Lattimer, J. M., et al. 2018, PhRvL, 121, 091102, doi: 10.1103/PhysRevLett.121.091102
- Dommes, V. A., & Gusakov, M. E. 2016, Mon. Not. Roy. Astron. Soc., 455, 2852, doi: 10.1093/mnras/stv2408
- Dong, J., Zuo, W., & Gu, J. 2015, Phys. Rev., C91, 034315, doi: 10.1103/PhysRevC.91.034315
- Fernandez, R., & Metzger, B. D. 2016, Annual Review of Nuclear and Particle Science, 66, 23, doi: 10.1146/annurev-nucl-102115-044819
- Finn, L. S. 1987, Mon. Not. Roy. Ast. Soc., 227, 265, doi: 10.1093/mnras/227.2.265
- Fischer, T., Bastian, N.-U. F., Wu, M.-R., et al. 2017a, ArXiv e-prints. https://arxiv.org/abs/1712.08788
- Fischer, T., Bastian, N.-U., Blaschke, D., et al. 2017b, Pub. Ast. Soc. Aus., 34, e067, doi: 10.1017/pasa.2017.63
- Flores, C. V., & Lugones, G. 2014, Class. Quant. Grav., 31, 155002, doi: 10.1088/0264-9381/31/15/155002
- Friedman, J. L., & Schutz, B. F. 1975, Astrophys. J. Lett., 199, L157, doi: 10.1086/181872
- Fu, W.-j., Bai, Z., & Liu, Y.-x. 2017, arXiv e-prints, arXiv:1701.00418. https://arxiv.org/abs/1701.00418

- Gandolfi, S., Carlson, J., & Reddy, S. 2012, Phys. Rev., C85, 032801, doi: 10.1103/PhysRevC.85.032801
- Glendenning, N. K. 1992, Phys. Rev. D, 46, 1274, doi: 10.1103/PhysRevD.46.1274
- Gomes, R. O., Char, P., & Schramm, S. 2019, ApJ, 877, 139, doi: 10.3847/1538-4357/ab1751
- Gregorian, P. 2015, Masters Thesis
- Heiselberg, H., & Pethick, C. J. 1993, Phys. Rev., D48, 2916, doi: 10.1103/PhysRevD.48.2916
- Hu, J., Bao, S., Zhang, Y., et al. 2020, Progress of Theoretical and Experimental Physics, 2020, doi: 10.1093/ptep/ptaa016
- Kantor, E. M., & Gusakov, M. E. 2014, Mon. Not. Roy. Astron. Soc., 442, 90, doi: 10.1093/mnrasl/slu061
- Klähn, T., & Fischer, T. 2015, Astrophys. J., 810, 134, doi: 10.1088/0004-637X/810/2/134
- Klähn, T., Fischer, T., & Hempel, M. 2017, Astrophys. J., 836, 89, doi: 10.3847/1538-4357/836/1/89
- Klevansky, S. 1992, Rev. Mod. Phys., 64, 649, doi: 10.1103/RevModPhys.64.649
- Krastev, P. G., & Li, B.-A. 2019, Journal of Physics G Nuclear Physics, 46, 074001, doi: 10.1088/1361-6471/ab1a7a
- Kruger, C. J., Ho, W. C. G., & Andersson, N. 2015, Phys. Rev., D92, 063009, doi: 10.1103/PhysRevD.92.063009
- Lai, D. 1994, Mon. Not. Roy. Astron. Soc., 270, 611, doi: 10.1093/mnras/270.3.611
- —. 1999, Mon. Not. Roy. Astron. Soc., 307, 1001, doi: 10.1046/j.1365-8711.1999.02723.x
- Lattimer, J. M., Li, A., Li, B.-A., & Xu, F. 2019, AIP Conference Proceedings, 2127, 020001, doi: 10.1063/1.5117791
- Lattimer, J. M., Pethick, C. J., Prakash, M., & Haensel, P. 1991, Phys. Rev. Lett., 66, 2701, doi: 10.1103/PhysRevLett.66.2701
- Li, C.-M., Yan, Y., Geng, J.-J., Huang, Y.-F., & Zong,H.-S. 2018, Phys. Rev., D98, 083013,doi: 10.1103/PhysRevD.98.083013
- Malik, T., Alam, N., Fortin, M., et al. 2018, PhRvC, 98, 035804, doi: 10.1103/PhysRevC.98.035804
- McDermott, P. N. 1990, Mon. Not. Roy. Ast. Soc., 245, 508Meszaros, P., & Rees, M. J. 1992, ApJ, 397, 570, doi: 10.1086/171813
- Miniutti, G., Pons, J. A., Berti, E., Gualtieri, L., & Ferrari, V. 2003, Mon. Not. Roy. Astron. Soc., 338, 389, doi: 10.1046/j.1365-8711.2003.06057.x
- Nandi, R., & Char, P. 2018, Astrophys. J., 857, 12, doi: 10.3847/1538-4357/aab78c

- Paschalidis, V., Yagi, K., Alvarez-Castillo, D., Blaschke,D. B., & Sedrakian, A. 2018, Phys. Rev., D97, 084038,doi: 10.1103/PhysRevD.97.084038
- Passamonti, A., Andersson, N., & Ho, W. C. G. 2016, Mon. Not. Roy. Astron. Soc., 455, 1489, doi: 10.1093/mnras/stv2149
- Prakash, M., Ainsworth, T. L., & Lattimer, J. M. 1988,Phys. Rev. Lett., 61, 2518,doi: 10.1103/PhysRevLett.61.2518
- Pratten, G., Schmidt, P., & Hinderer, T. 2020, Nature Communications, 11, 2553, doi: 10.1038/s41467-020-15984-5
- Radice, D., Perego, A., Zappa, F., & Bernuzzi, S. 2018, Astrophys. J., 852, L29, doi: 10.3847/2041-8213/aaa402
- Ranea-Sandoval, I. F., Guilera, O. M., Mariani, M., & Orsaria, M. G. 2018, J. Cosmol. Astropart. Phys., 2018, 031, doi: 10.1088/1475-7516/2018/12/031
- Reisenegger, A., & Goldreich, P. 1992, ApJ, 395, 240, doi: 10.1086/171645
- —. 1994, ApJ, 426, 688, doi: 10.1086/174105
- Reyes, S., & Brown, D. A. 2020, ApJ, 894, 41, doi: 10.3847/1538-4357/ab64e8
- Sahoo, B., Chakraborty, S., & Sahoo, S. 2016, Physics of Atomic Nuclei, 79, 1, doi: 10.1134/S1063778816010178
- Sieniawska, M., Turczański, W., Bejger, M., & Zdunik, J. L. 2019, Astron. Astrophys., 622, A174, doi: 10.1051/0004-6361/201833969
- Sotani, H., Maruyama, T., & Tatsumi, T. 2013, Nucl. Phys., A906, 37, doi: 10.1016/j.nuclphysa.2013.03.011
- Sotani, H., Yasutake, N., Maruyama, T., & Tatsumi, T. 2011, Phys. Rev., D83, 024014, doi: 10.1103/PhysRevD.83.024014

- Strohmayer, T. E. 1992, in American Astronomical Society Meeting Abstracts #180, Vol. 180, 38.03
- Tews, I., Margueron, J., & Reddy, S. 2018, Phys. Rev., C98, 045804, doi: 10.1103/PhysRevC.98.045804
- van Dalen, E., Fuchs, C., & Faessler, A. 2004, Nuclear Physics A, 744, 227 ,
 - doi: https://doi.org/10.1016/j.nuclphysa.2004.08.019
- Vásquez Flores, C., & Lugones, G. 2014, Classical and Quantum Gravity, 31, 155002, doi: 10.1088/0264-9381/31/15/155002
- Wei, W., Irving, B., Salinas, M., Klhn, T., & Jaikumar, P. 2019, The Astrophysical Journal, 887, 151, doi: 10.3847/1538-4357/ab53ea
- Weinberg, N. N. 2016, Astrophys. J., 819, 109, doi: 10.3847/0004-637X/819/2/109
- Wilson, P. S., & Roy, R. A. 2008, American Journal of Physics, 76, 975
- Wiringa, R. B., Fiks, V., & Fabrocini, A. 1988, Phys. Rev. C, 38, 1010, doi: 10.1103/PhysRevC.38.1010
- Wood, A. B. 1930, A Textbook of Sound (New York: MacMillan)
- Xu, W., & Lai, D. 2017, Phys. Rev. D, 96, 083005
- Yang, H., Paschalidis, V., Yagi, K., et al. 2018, Phys. Rev. D, 97, 024049, doi: 10.1103/PhysRevD.97.024049
- Yu, H., & Weinberg, N. N. 2017, Mon. Not. Roy. Astron. Soc., 470, 350, doi: 10.1093/mnras/stx1188
- Yu, H., & Weinberg, N. N. 2017, MNRAS, 464, 2622, doi: 10.1093/mnras/stw2552
- Zhang, N.-B., & Li, B.-A. 2019, European Physical Journal A, 55, 39, doi: 10.1140/epja/i2019-12700-0
- Zhou, Y., & Zhang, F. 2017, ApJ, 849, 114, doi: 10.3847/1538-4357/aa906e
- Zhu, Z.-Y., Zhou, E.-P., & Li, A. 2018, Astrophys. J., 862, 98, doi: 10.3847/1538-4357/aacc28